

An open-source implementation and validation of 5G NR Configured Grant for URLLC in ns-3 5G LENA: a scheduling case study in Industry 4.0 scenarios

Ana Larrañaga^a, M. Carmen Lucas-Estañ^b,

Sandra Lagen^c, Zoraze Ali^c, Imanol Martinez^a, Javier Gozalvez^b

^a*HW and Communication Systems Area, Ikerlan Technology Research Centre, Mondragón 20500, Spain*

^b*UWICORE Laboratory, Universidad Miguel Hernández de Elche (UMH), Elche 03202, Spain*

^c*Centre Tecnològic de Telecomunicacions de Catalunya (CTTC/CERCA), Castelldefels, Barcelona, Spain*

Abstract Factories are undergoing a digital transformation towards more cost-efficient, zero-defect manufacturing. The digitalized factories require communication networks capable to satisfy their strict latency and reliability demands. 5G and beyond networks are being designed to efficiently support services demanding Ultra-Reliable and Low Latency Communications (URLLC). At the MAC level, the use of dynamic scheduling for uplink transmissions entails a non-negligible latency introduced by the signaling exchanged to request and inform about the radio resources allocated for each packet transmission. To reduce the transmission latency, 5G defines Configured Grant (CG) for UL transmissions that pre-allocates radio resources to the User Equipments (UEs) and eliminates the need for requesting resources for each transmission. In this context, the availability of 5G NR simulation tools that accurately implement all 5G NR functionalities, and in particular, the technological enablers introduced in 5G NR to support URLLC, is critical to analyze the capability of 5G and beyond networks to support time-critical services and research on new solutions. The availability and access to such tools is limited and, to the best of the author's knowledge, there are currently no open-source 5G NR simulators that implement configured grant in 5G NR. To overcome this issue, this work presents the first implementation of configured grant in an open-source 5G NR simulator. In particular, configured grant has been implemented in the ns-3 5G-LENA system-level simulator, and it is publicly available. To accurately model the flexibility of 5G NR, we have also improved the implementation of Orthogonal Frequency Division Multiple Access (OFDMA) access mode in 5G-LENA according to 5G NR. To validate the implementation of CG and analyze the capability of 5G NR to support time-critical services, we analyze the latency performance that can be achieved using CG with different scheduling policies in Industry 4.0 scenarios. The results show that the latency values achieved with CG in 5G-LENA match with those reported by previous analytical studies. In addition, this study shows the importance of efficiently using radio resources to reduce the latency experienced and meet the requirements of critical services.

Keywords: 5G, Configured Grant, Grant-free scheduler, scheduling, software simulation, URLLC, ns-3, 5G-LENA

1. Introduction

Factories are undergoing a digital transformation towards more cost-efficient, zero-defect manufacturing environments capable to flexibly adapt to changes in production and demand [1]. Industrial applications such as digital twins, motion control, or control-to-control communications demand strict latency and cycle times requirements ranging from milliseconds to microseconds [2] [3]. They require communication networks capable of satisfying their communication requirements. 5G networks are designed to support ultra-reliable and low-latency communications (URLLC). In fact, 5G and its future evolution are considered critical enablers for Industry 4.0 paradigm. 5G introduces several mechanisms at the PHY and MAC layers to reduce latency. For example, 5G includes flexible numerologies with different slot durations (from 1 ms to 0.0625 ms) and mini-slot transmissions. In addition to dynamic scheduling, 5G introduces semi-static scheduling to

reduce communication latency. With dynamic scheduling, the base station or gNB informs the UEs about the radio resources used for each packet transmitted in downlink (DL) before the transmission of each packet. When a UE has a packet to transmit in uplink (UL), the UE requests the gNB for resources, and the gNB replies with a grant and the information about the allocated resources. This process introduces a non-negligible transmission delay, which is higher in UL to the higher number of messages exchanged between the UE and the gNB. Semi-static scheduling (referred to as configured grant or CG for UL transmissions and semi-persistent scheduling or SPS for DL transmissions) pre-allocates radio resources periodically to UEs [4], and UEs can transmit in the pre-allocated resources as soon as they have data to transmit. Semi-static scheduling eliminates the latency introduced by requesting radio resources for each transmission.

Availability and access to accurate simulation tools are critical to analyze the capability of 5G NR to support critical

industrial services and research new solutions. However, to the best of the author's knowledge, there are currently no open-source 5G NR simulators that implement configured grant in 5G NR, which is critical for URLLC services. To overcome this issue, this work presents the first implementation of configured grant in an open-source 5G NR simulator. In particular, configured grant has been implemented in 5G-LENA [5]. 5G-LENA is an open-source discrete-event network simulator of the 5G NR based on ns-3 [6]. 5G-LENA implements most of the main 5G NR functionalities, such as the NR frame structures, the numerologies, or bandwidth parts (BWPs). However, 5G-LENA does not implement configured grant scheduling. The code of the configured grant implementation for 5G-LENA is publicly available in [7] and it uses the ns-3 version available in [8].

The latency performance achievable with CG strongly depends on the multiple access scheme since it establishes how radio resources can be shared by the UEs and determines the flexibility of the scheduler to allocate radio resources to the UEs. It is then necessary to accurately model the OFDMA multiple access scheme used in 5G NR in order to analyze the actual capability of 5G NR using CG. 5G-LENA implements several multiple access schemes, but none of them models the flexibility of OFDMA that allows simultaneous sharing of radio resources in the time and frequency domain. In this context, we have also implemented OFDMA in 5G-LENA according to 5G NR.

To validate the implementation of CG and analyze the capability of 5G NR to support critical industrial services, we consider a scheduling case study in an Industry 4.0 scenario. In particular, this work analyzes the latency performance that can be achieved using CG with different scheduling policies. The results show that the latency values achieved with CG in 5G-LENA match with those reported by previous analytical studies. In addition, the results highlight the importance of making efficient use of radio resources to reduce the latency experienced and meet the requirements of critical services.

The rest of the paper is organized as follows. 5G New Radio is presented in Section II, and Section III describes the 5G-LENA network simulator. Section IV presents the implementation of CG in 5G-LENA. Section IV also presents the modifications done in 5G-LENA to accurately model OFDMA and the scheduling policies used to evaluate the performance of CG. Section V describes the evaluation scenario and the schemes used as a reference. In Section VI, we derive analytical expressions of the maximum latency experienced with CG and the different scheduling policies. We compare in Section VI the latency achieved analytically and by simulation to validate the implementation of CG. Section VII presents the performance results. Section VIII concludes the paper.

2. 5G New Radio

5G uses OFDM (Orthogonal Frequency Division Multiplexing) and radio resources are organized in Resource Blocks (RBs) in the frequency domain and in slots in the time domain. A radio resource is composed of an RB, which contains 12 consecutive slots subcarriers, and an OFDM symbol. 5G defines the use of flexible numerologies. A numerology μ is given by the use of a Subcarrier Spacing (SCS) and a slot duration. Numerologies μ from 0 to 4 use a SCS equal to 15, 30, 60, 120 and 240 kHz SCS respectively [9]. The slot duration is given by $1/2^\mu$ ms, which results in slot durations from 1 ms for $\mu=0$ to 0.0625 ms for $\mu=4$. Slots are organized in frames of 10 ms. A slot consists of 14 OFDM symbols in the time domain when the normal cyclic prefix (CP) is used (the normal CP can be used with all the numerologies). An extended CP can also be used with $\mu=2$. In this case, a slot consists of 12 OFDM symbols. Numerologies 0, 1, and 2 can be used in the lower frequency range (410 MHz-7.125 GHz), and numerologies 2, 3, and 4 can be used in the higher frequency range (24.25 GHz-52.6 GHz). 5G NR allows transmissions to start at any OFDM symbol within a slot and to use only the number of symbols needed for the transmission. This results in mini-slot transmissions when transmissions only use part of the symbols of a slot, or full-slot transmissions when all the symbols are used. The use of mini-slot transmissions can even reduce the latency.

5G can use frequency-division duplex (FDD) or time-division duplex (TDD) modes. On the one hand, TDD provides high flexibility as each slot in a frame can be configured for UL or DL transmissions. Furthermore, a single slot can be split into segments of consecutive symbols that can be used for UL or DL [10]. On the other hand, FDD organizes UL and DL transmissions on separated frequencies. FDD can reduce the communication latency since resources are always available simultaneously for UL and DL transmissions.

5G NR uses Low Density Parity Check coding with Quadrature Phase Shift Keying (QPSK), 16 Quadrature Amplitude Modulation (QAM), 64 QAM, or 256 QAM for data channels. 5G NR defines three Modulation and Coding Scheme (MCS) tables that provides different trade-off between spectrum efficiency and protection against error. MCS tables 1 and 2 guarantee a BLER of 10%, and MCS table 3 guarantees a BLER of 10^{-5} when used according to the CQI tables defined in [11].

5G NR uses Orthogonal OFDMA multiple access scheme that allows UEs to share radio resources in the frequency and time domains. With OFDMA, an RB can be used by different UEs in different OFDM symbols, and different RBs in the same OFDM symbol can be used by different UEs. As a result, UEs can receive any number of OFDM symbols and RBs. Transmissions in 5G NR can be performed using dynamic or semi-static scheduling in both UL and DL [12]. With dynamic scheduling, the gNB allocates resources dynamically for each packet transmission. When a packet is

generated in DL for a UE, the gNB sends a control message to inform the UE about the allocated radio resources. When a UE needs to transmit a packet in UL, the UE sends a scheduling request (SR) to the gNB. The gNB then replies with a grant message to the UE with the information about the radio resources to use for the packet transmission. The UE transmits the packet together with the buffer status report (BSR) to inform the gNB if it has more data to transmit. If this is the case, the gNB will allocate radio resources for a new transmission and will inform the UE. This process is repeated while the UE has pending data to transmit. Dynamic scheduling makes efficient use of radio resources. However, the signaling exchange between the UE and the gNB before the packet transmission can increase the latency of the transmission. This is more critical for UL transmissions since the amount of signaling between the UE and the gNB is higher. This cannot be appropriate for latency-critical industrial applications. Semi-static scheduling can also be used for packet transmission in 5G NR: SPS in DL and CG in UL. CG and SPS pre-assign radio resources periodically to the UEs before the packets are generated. When a data packet is generated, the packet can be transmitted in the pre-allocated resources. CG and SPS avoid the signaling exchange between the UE and the gNB to request/inform about the allocated radio resources, reducing the transmission latency. The gNB informs the UEs about the pre-allocated radio resources and their periodicity using Radio Resource Control (RRC) signaling during the connection establishment. Two types of CG are defined in [12]: type 1, which activates the configured uplink grant from the moment it is configured, and type 2, where the grant is activated or deactivated using DL control messages. CG type 1 is illustrated in Figure 1.

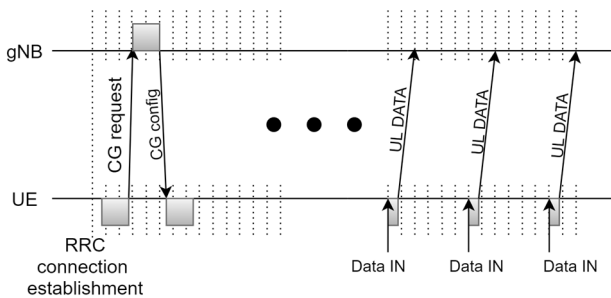


Figure 1. Configured grant type 1.

3. 5G-LENA network simulator

5G-LENA is an open-source discrete-event network simulator of the 5G NR [5] implemented over ns-3. ns-3 is an open C++ simulation environment for networking research that offers a solid simulation core that supports research on both IP and non-IP-based networks. 5G-LENA is the evolution of LENA that was initially developed to implement the RAN and the core network of Long Term Evolution

(LTE). The efforts on the development of 5G-LENA focused first on the RAN. 5G-LENA implements the fundamental PHY-MAC NR features in line with the NR specifications [12].

5G-LENA implements two main C++ classes to simulate the functionalities of the gNB (NrGnb class) and the UE (NrUe class) (see Figure 2). For the gNB and the UE, 5G-LENA models the different layers of the protocol stack: PHY, MAC, Radio Link Control (RLC), Packet Data Convergence Protocol (PDCP), and RRC. The upper layers RLC, PDCP, and RRC currently rely on LTE LENA implementation. The PHY and MAC layers implement the main NR features. For example, the PHY layer implements the flexible frame structure defined in [12] for 5G NR. Both TDD and FDD duplexing modes can be configured. In TDD, slots can be flexibly configured for DL or UL transmissions as established by 5G 3GPP standard. 5G-LENA also allows flexibly configuring the number of OFDM symbols within a slot to be used for UL and DL transmissions. The 5G-LENA PHY layer considers the use of the new numerologies defined in [12] for 5G NR, both normal and extended CP, and the different modulation and coding schemes defined in [11]. Two beamforming methods have been added, long-term covariance matrix and beam-search, using either ideal beamforming or realistic beamforming based on uplink Sounding Reference Signals [13]. Recently, dual-polarized MIMO for the downlink has been implemented [14]. 5G-LENA also supports different channel and propagation models according to the 3GPP spatial channel model defined in TR 38.901 [15]. Moreover, it has been recently calibrated in outdoor 3GPP reference scenarios [16].

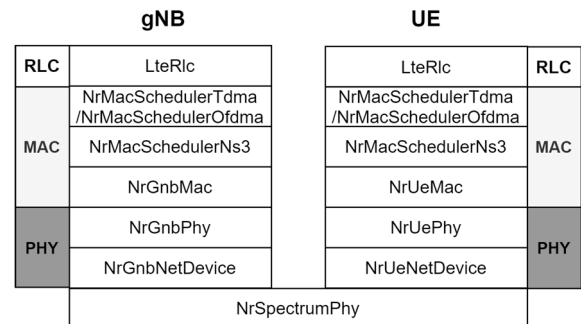


Figure 2. Logical representation of the 5G-LENA RAN class.

5G-LENA has also evolved the MAC to support 5G NR. 5G-LENA supports three different multiple access schemes: TDMA, OFDMA, and OFDMA with variable TTI [17]. With TDMA, UEs access radio resources at different OFDM symbols and all RBs in a symbol must be assigned to the same UE. This is shown in Figure 3.a. . Figure 3 shows how radio resources are shared by different UEs when the different multiple access schemes are used. Figure 3 depicts the time-frequency resource grid for a slot made up of 14 OFDM symbols in time and R_{BW} number of RBs in the frequency

domain. Squares in Figure 3 represent an OFDM symbol in the time domain and one RB in the frequency domain. The first and last symbols are reserved for DL and UL CTRL channels. In this example, each UE needs 4 RBs to transmit its packet. Colored squares represent the RBs assigned to UEs for packet transmission. Figure 3.a shows that although UEs only require 4 radio resources to transmit their packets, they receive all the RBs (R_{BW}) in an OFDMA symbol. OFDMA multiple access mode implemented in current version of 5G-LENA is a constrained version of OFDMA in 5G NR. OFDMA implemented in 5G-LENA allocates an RB in all the OFDM symbols within a slot to the same UE. Different UEs can access to different RBs. This is shown in Figure 3.b. The third multiple access scheme implemented in 5G-LENA is referred to as OFDMA with variable TTI. It allows dividing the OFDM symbols within a slot into two or more segments with a different or equal number of OFDM symbols. The radio resources within each of these segments can be accessed by the UEs assigned to the same antenna beam. In each of these segments, OFDMA multiple access schemes implemented in 5G-LENA is applied (see Figure 3.c).

None of these multiple access schemes accurately model the flexibility offered by OFDMA in 5G NR. OFDMA allows to allocate different number of RBs and OFDM symbols to

UEs. An example is shown in Figure 3.d. The TDMA and OFDMA schemes currently implemented in 5G-LENA are constrained to allocate a number of radio resources that is multiple of R_{BW} (the number of available RBs in a particular bandwidth) or S_{slot} (that represents the number of OFDM symbols reserved for UL data transmission within a slot) respectively. In the case of OFDMA with variable TTI, the number of radio resources allocated to UEs is multiple of the number of OFDM symbols within a segment. OFDMA in 5G NR allows adjusting the number of assigned resources more accurately to the UEs' demand. This allows more efficient use of radio resources .

5G-LENA implements dynamic scheduling in DL and UL; semi-static scheduling is not yet implemented in 5G-LENA. Different scheduling policies are currently implemented, such as round-robin, proportional fair, etc, but other policies can also be included. It is important to note that a UE receives a number r of RBs in s consecutive OFDM symbols, i.e., a UE receives $r \times s$ radio resources. Due to interference model limitations in 5G-LENA, if two UEs receive RBs in the same OFDM symbol, the two UEs must receive RBs in the same number s of OFDM symbols [5]. Finally, 5G-LENA allocates radio resources for UL transmissions from the last symbol to the first within a slot.

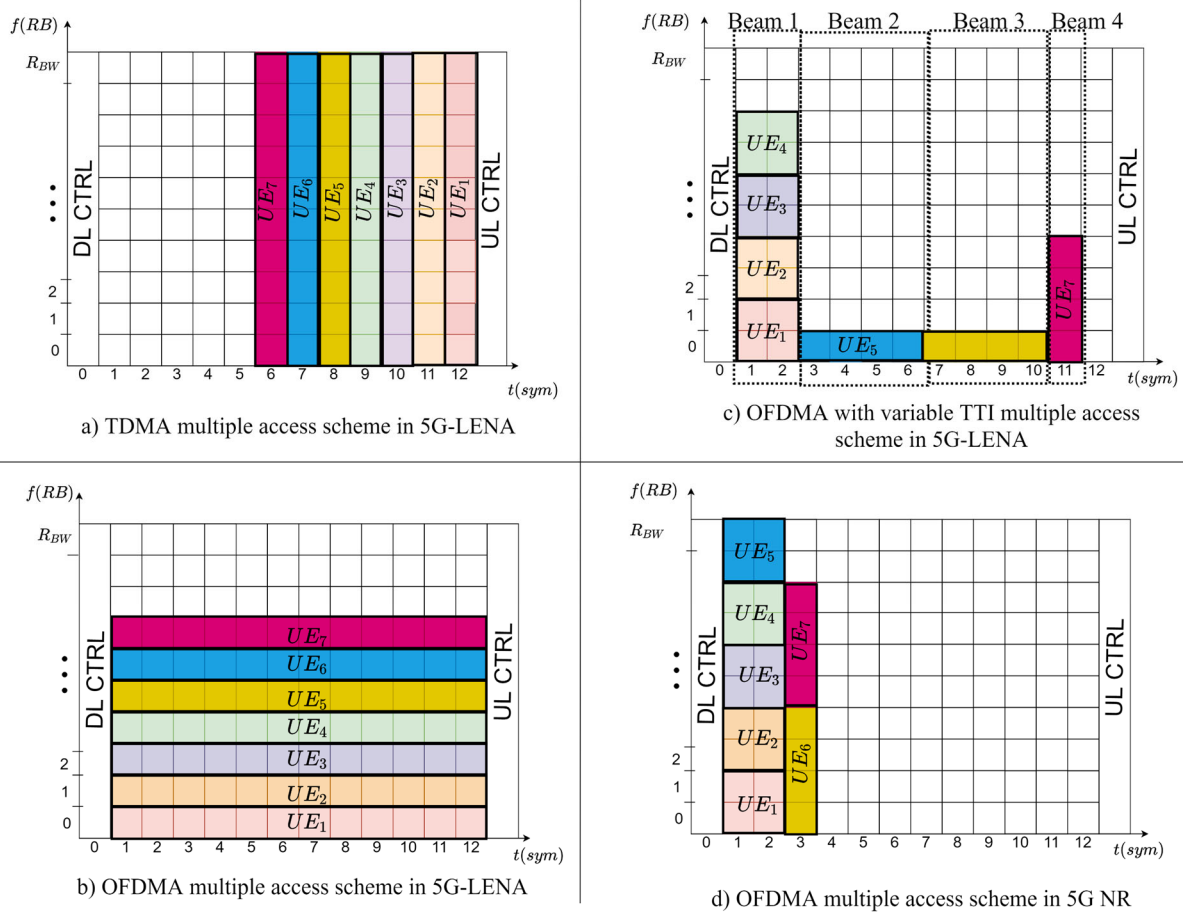


Figure 3. Example of radio resource allocation with the different multiple access modes.

4. Implementation of Configured Grant in 5G-LENA

4.1. Configured Grant

5G-LENA has been extended in this work to simulate UL transmissions using configured grant. We have implemented configured grant Type 1 that configures and stores the UL grant at the session establishment. Configured grant Type 1 avoids potential delays that might be introduced in the activation/deactivation of the configured UL grant. It results more suitable for services with stringent latency requirements.

Configured grant has been implemented in 5G-LENA using a state machine that is presented in Figure 4. The state machine is implemented at the UE to manage UL transmissions. `INACTIVE_CG` is the initial state and is activated for each UE when the simulation starts. A UE requests a configured UL grant to the UE when a new RRC connection is established. To this end, the UE prepares a CG request (CGR) with the Radio Network Temporary Identifier (RNTI), the size of the packets to transmit and the packet periodicity. The CGR is generated at the MAC layer and is sent to the PHY layer to be transmitted. At this moment, the UE changes to `TO_SEND_CG` state. The UE transmits the CGR to the gNB in the next slot, and changes to `TO_RECEIVE_CG` state. When the gNB receives the CGR, it allocates radio resources periodically for the UE according to the traffic information received and a scheduling policy. The gNB generates the *ConfiguredGrantConfig* message [18] with the configured UL grant and information about the pre-allocated radio resources. The gNB transmits the *ConfiguredGrantConfig*

message to the UE. When the UE receives the CG, it stores the configured UL grant and changes to `ACTIVE_CG` state. The UE checks if it is in `ACTIVE_CG` state (that means it has a configured UL grant) each time a new data packet is generated. If this is the case, the UE changes to `SCH_CG_DATA`. The UE prepares the data packet to be transmitted and changes to `ACTIVE_CG` state. The packet is then transmitted to the gNB on the pre-allocated resources. The gNB waits to receive data packets from the UE on the pre-allocated resources.

4.2. Flexible Multiple Access and Radio Resource Allocation

Flexibility in radio resource allocation is constrained by the multiple access scheme used in the system. OFDMA in 5G NR allows UEs to share radio resources in the time and frequency domain. However, none of the multiple access schemes implemented in 5G-LENA implement the real capabilities of OFDMA in 5G NR. The TDMA, OFDMA and OFDMA with variable TTI multiple access schemes currently implemented in 5G-LENA establish restrictions on sharing radio resources in frequency or time among different UEs (see Section 0). The constraints introduced by the multiple access schemes implemented in 5G-LENA may result in an inefficient use of radio resources. UEs may receive a higher number of radio resources than they actually need. This is especially the case when traffic is characterized by small packet sizes. This can lead to higher latencies that can be detrimental to time-critical services.

We have extended the 5G-LENA MAC layer to implement a more accurate version of OFDMA in 5G NR. The objective is to provide an open software tool that accurately emulates the actual features and capabilities of 5G NR to support latency-critical services. The new OFDMA implemented in 5G-LENA allows allocating r RBs in s consecutive OFDM symbols to a UE, with r and s being any integer number in $[1, R_{BW}]$ and $[1, S_{slot}]$, respectively (s is always equal to S_{slot} with the current implementation of OFDMA in 5G-LENA, and r is equal to R_{BW} with TDMA).

The new implementation of OFDMA is included in the `DoScheduleUIData` function in the MAC layer of the gNB in 5G-LENA. This function executes the radio resource allocation process for UL transmissions and is executed by the gNB after receiving a CGR. Figure 5 illustrates the operation of the `DoScheduleUIData` function. This function first decides the number of OFDM symbols and RBs that should be allocated to each UE that has requested for a configured UL grant. This decision is implemented in the `AssignULRBG` function. The number of OFDM symbols and RBs allocated to each UE depends on several factors. First, it depends on the amount of data to transmit by the UE and the MCS to use in the packet transmission. The decision is also subject to the multiple access scheme. In this context, the `AssignULRBG` function has been modified to allow

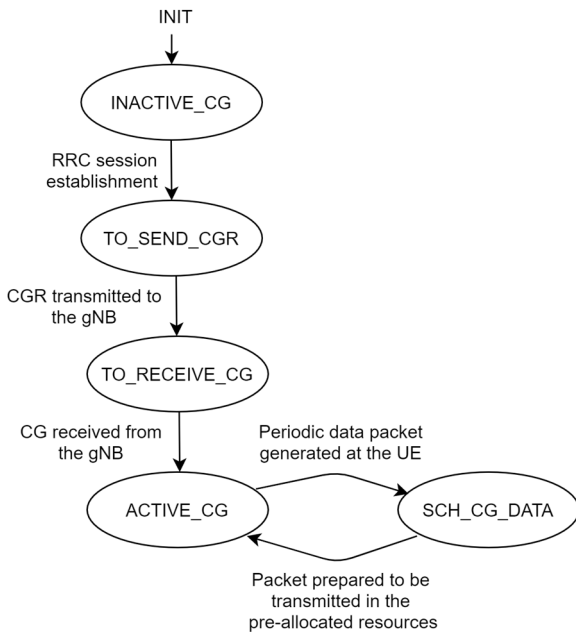


Figure 4: Configured grant state machine.

sharing radio resources among different UEs simultaneously in frequency and time according to OFDMA in 5G NR. The final radio resource allocation depends on the particular scheduling policy implemented. The messages to inform the UEs are created after the radio resource allocation decision is taken. When configured grant is used for UL transmissions, the CreateUICGConfig function is called. CreateUICGConfig is a new function that generates the control message with the configured grant scheduling information for each UE.

Finally, we have also modified the order followed in 5G-LENA to allocate radio resources for UL transmissions within a slot. As presented in section III, radio resources are allocated from the last to the first symbol within a slot in 5G-LENA. This order is not established in 5G NR. Therefore, we have eliminated this condition. Resources can now be allocated from the first to the last symbol within a slot, which is also key to guarantee very low latency.

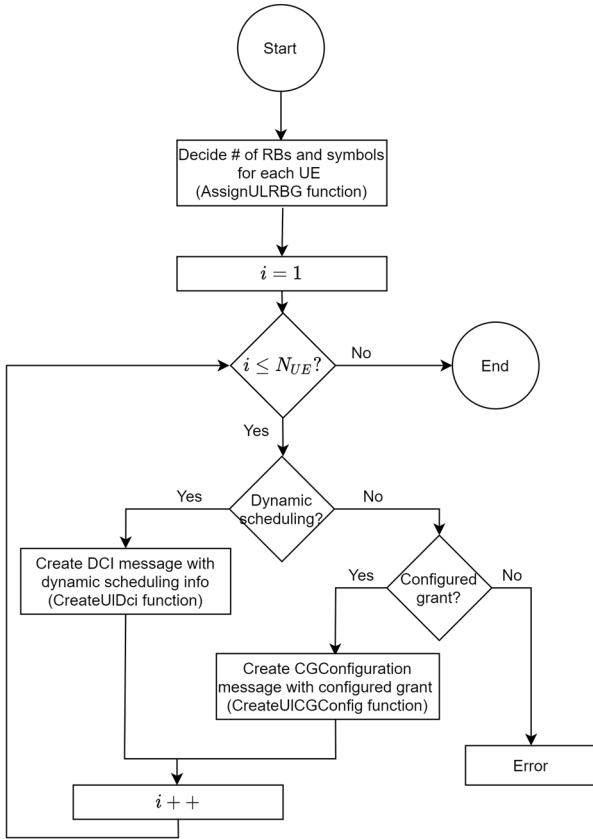


Figure 5. Radio resource allocation process for UL transmissions (DoScheduleUIData function) in 5G-LENA.

4.3. Scheduling Policies

Two new scheduling policies have been implemented in 5G-LENA to be applied with CG. These scheduling policies exploit the flexibility of OFDMA in 5G NR. The designed scheduling policies decide the number r_i of RBs and number s_i of OFDM symbols allocated to each UE $_i$, with $i \in \mathbb{N}$ and $i \in [1, N_{UE}]$. Both scheduling schemes aim to use radio resources efficiently and minimize the experienced latency. To this end, they try to allocate the lowest number of radio resources that satisfies the radio resource demand of each UE. The defined scheduling policies aim to show the importance of accurately emulating the capabilities and flexibility of 5G NR, and they do not search for optimal solutions. This flexibility can be exploited to increase performance and more efficiently support latency-critical services.

The first scheduling policy minimizes the number of OFDM symbols allocated to each UE, referred to as Sym-OFDMA scheduler. The operation of Sym-OFDMA is presented in Algorithm I. Sym-OFDMA serves UEs following a first-come, first-served basis, i.e., from UE $_1$ to UE $_{N_{UE}}$ (line 3 in Algorithm I). Sym-OFDMA allocates radio resources from the first to the last symbol within a slot (variables n_{slot} , n_{sym} and n_{RB} represent the current slot, symbol within the slot, and RB respectively that is currently being allocated to a UE). Each UE $_i$ demands d_i radio resources that is calculated as a function of the size of the packet to transmit and the MCS to use in the packet transmission. If the number d_i of radio resources demanded by a UE $_i$ is equal to or lower than R_{BW} (the number of RBs in a symbol), UE $_i$ receives d_i consecutive RBs in an OFDM symbol, i.e., $r_i = d_i$ and $s_i = 1$ (see lines 4-5 in Algorithm I). $r_{ini,i}$ and $s_{ini,i}$ represent the first RB and OFDM symbol, respectively, allocated to UE $_i$ (see line 16). If the UE $_i$ demands more than R_{BW} radio resources ($d_i > R_{BW}$), UE $_i$ receives R_{BW} RBs in $\lceil d_i / R_{BW} \rceil$ consecutive OFDM symbols (line 7 in Algorithm I). UE $_{i+1}$ will receive RBs in the same OFDM symbol as UE $_i$ if the number of unallocated RBs are enough to satisfy the demand of UE $_{i+1}$ (see lines 15-16). Otherwise, UE $_{i+1}$ will receive RBs in the next OFDM symbol (lines 9-11). Sym-OFDMA also considers that a UE can only receive RBs within a slot. In case there are not enough unallocated RBs and symbols to meet d_i in the current slot, the UE $_i$ will be served in the next slot (lines 12-14). Figure 6.a shows an example of the radio resource allocation done by Sym-OFDMA in a scenario where 7 UEs demand 4 radio resources each to transmit using configured grant. Figure 6 represents the radio resources in one slot of 14 OFDM symbols, where the first and last symbols are reserved for control signals, and bandwidth is divided in $R_{BW}=10$ RBs.

ALGORITHM I: *SYM-OFDMA*

1. Input: $d_i \forall i \in [1, N_{UE}]$
 2. $n_{slot}=1, n_s=1, n_{RB}=1$
 3. **For** $i=1$ to N_{UE}
 4. **If** $d_i \leq R_{BW}$
 5. $r_i=d_i, s_i=1$
 6. **Else**
 7. $r_i=R_{BW}, s_i=[d_i/R_{BW}]$
 8. **End If**
 9. **If** $R_{BW} - n_{RB} + 1 < r_i$
 10. $n_{RB}=1, n_s=n_s+1$
 11. **End If**
 12. **If** $n_s + s_i - 1 > S_{slot}$
 13. $n_{slot}=n_{slot}+1, n_s=1, n_{RB}=1$
 14. **End If**
 15. $r_{ini,i}=n_{RB}, s_{ini,i}=n_s, slot_i=n_{slot}$
 16. $n_{RB}=n_{RB}+r_{ini,i}$
 17. **End For**
-

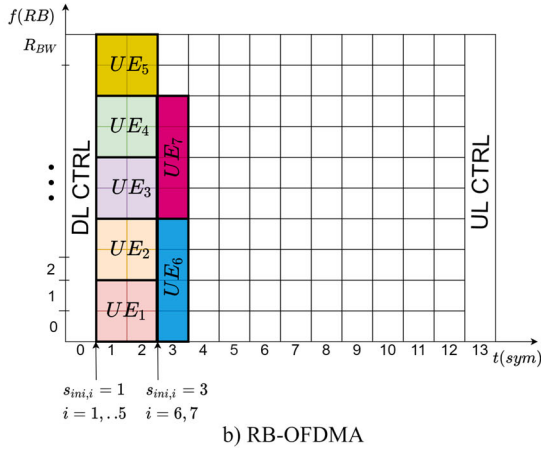
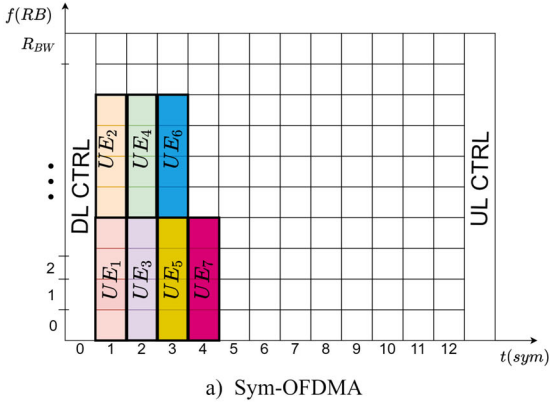


Figure 6. Radio resource allocation with the designed scheduling policies.

The second scheduling policy calculates the number of radio resources (r_i) and OFDM symbols (s_i) that should be allocated to each UE_i to minimize the number of RBs that are not allocated to UEs. It also establishes that each UE_i has to receive at least r_{min} RBs (r_{min} can take any integer number between 1 and R_{BW}^1). This second scheduling policy is referred to as RB-OFDMA. The operation of RB-OFDMA is presented in Algorithm II. RB-OFDMA also serves UEs following a first-come, first-served order, and allocates radio resources from the first to the last symbol within a slot. RB-OFDMA distributes the R_{BW} RBs in a symbol among the maximum number of UEs (n_{UE}) considering that $r_i \geq r_{min}$ for each UE_i , i.e., $n_{UE}=\lfloor R_{BW}/r_{min} \rfloor$ (line 3 of Algorithm II). The UEs are divided in sets of n_{UE} UEs (line 5); the last set of UEs can have less than n_{UE} . The UEs in each set ϕ will share the RBs in the same OFDM symbols. If the number of UEs in a set ϕ is equal to n_{UE} , each UE_i in ϕ will receive $r_i=r_{min}$ RBs (lines 7 and 8). If the number of UEs in a set ϕ is lower than n_{UE} , the first $(n_{UE}/n)-\lfloor n_{UE}/n \rfloor \cdot n$ UEs in ϕ will receive $r_i=\lfloor n_{UE}/n \rfloor \cdot r_{min}$ RBs (line 10). The rest of UEs in ϕ will receive $r_i=\lfloor n_{UE}/n \rfloor \cdot r_{min}$ RBs (line 11). Based on the number of RBs allocated to each UE, RB-OFDMA calculates the number d_i^S of OFDM symbols that each UE_i needs to meet

ALGORITHM II: *RB-OFDMA*

1. Input: $d_i \forall i \in [1, N_{UE}], r_{min}$
 2. $n_{slot}=1, n_s=1, n_{RB}=1, n_{UEwithRB}=0$
 3. Define $n_{UE}=\lfloor R_{BW}/r_{min} \rfloor$
 4. **While** there are UEs without resources
 5. Create set ϕ with $UE_i \forall i$ such that $i=[n_{UEwithRB}+1, \min(n_{UEwithRB}+n_{UE}, N_{UE})]$
 6. Define n =number of UEs in ϕ
 7. **If** $n=n_{UE}$
 8. $r_i=r_{min} \forall UE_i$ in ϕ
 9. **Else**
 10. $r_i=\lfloor \frac{n_{UE}}{n} \rfloor \cdot r_{min}$ for the first $(\frac{n_{UE}}{n} - \lfloor \frac{n_{UE}}{n} \rfloor) \cdot n$ UEs in ϕ
 11. $r_i=\lfloor \frac{n_{UE}}{n} \rfloor \cdot r_{min}$ for the last $n - (\frac{n_{UE}}{n} - \lfloor \frac{n_{UE}}{n} \rfloor) \cdot n$ UEs in ϕ
 12. **End If**
 13. **For** all UE_i in ϕ
 14. $d_i^S=d_i/r_i, r_{ini,i}=n_{RB}, n_{RB}=n_{RB}+r_i$
 15. **End For**
 16. $d^S=\max\{d_i^S\} \forall UE_i$ in ϕ
 17. $s_i=d^S \forall UE_i$ in ϕ
 18. **If** $n_s+n_s+d^S-1 > S_{slot}$
 19. $n_{slot}=n_{slot}+1, n_s=1$
 20. **End if**
 21. $s_{ini,i}=n_s, slot_i=n_{slot} \forall UE_i$ in ϕ
 22. $n_s=n_s+d^S, n_{RB}=1$
 23. $n_{UEwithRB}=n_{UEwithRB}+n_{UE}$
 24. **End While**
-
-

¹ r_{min} can be configured based on traffic characteristic to optimize system performance.

its demand d_i (line 14). Once d_i^S is known, all UEs in a group ϕ receive the number of RBs necessary to satisfy the UE that requires a greater number of OFDM symbols (lines 16-17). RB-OFDMA also considers that a UE can only receive RBs within a slot. In case there are not enough unallocated RBs and symbols to meet r_i and s_i in the current slot, the UE $_i$ will be served in the next slot (lines 18-20). Figure 6.b shows an example of the radio resource allocation done with RB-OFDMA. The example considers that 7 UEs demand 4 radio resources to transmit their data using configured grant and $r_{min}=2$. In this example, the N_{UE} UEs are divided in two sets of UEs. The first set includes 5 UEs (equal to $\lfloor R_{BW}/r_{min} \rfloor$) that receive $r_i=2$ RBs and $s_i=2$ OFDM symbols. The second set includes 2 UEs that receive $r_i=4$ RBs and $s_i=1$ OFDM symbols.

The value of r_{min} can be tuned to optimize radio resource efficiency. In this work, we calculate r_{min} with the aim of minimizing the number of RBs not allocated to any UE. To this end, we search the value of r_{min} that minimizes the number of not allocated RBs in a symbol (lines 1-6 of Algorithm III). If several values satisfy this condition, we select the value that provides the lowest difference between the number of allocated radio resources to UEs ($r_i \cdot s_i = x \cdot d_i^S(x)$) and their demands (line 8).

ALGORITHM III: r_{min} in RB-OFDMA

1. $aux=R_{BW}$
 2. Create $X=\{x\}$ with $x \in \mathbb{N}$, $1 < x < R_{BW}$, and $\text{mod}(aux/x)=0$.
 3. **If** X is empty
 4. $aux=aux-1$
 5. Go to 3
 6. **End If**
 7. Calculate number $d_i^S(x)$ of OFDM symbols needed to meet the UE demands d_i when UEs receives x RBs, $\forall i \in [1, N_{UE}]$ and $\forall x \in X$.
 8. Set $r_{min} = x \in X$ that satisfies $\min_{i,x} (x \cdot d_i^S(x) - d_i)$
-

5. Evaluation Scenario & Reference Schemes

We consider an evaluation scenario where a single 5G NR cell covers a typical work cell of $10 \times 10 \text{ m}^2$ where a closed-loop control application is implemented. The cell is assigned a bandwidth of BW in the 3.7–3.8 GHz band², with BW equal to 10, 20 or 40 MHz, and operates in TDD mode [19]. We consider slots with 14 OFDM symbols, and evaluate 3 slot configurations for which the last 13, 9 and 5 OFDM symbols are used for UL and the rest of OFDM symbols for DL. We refer to the different configurations as 1D13U, 5D9U, and 9D5U respectively. The first and last symbols within a slot are reserved for the transmission of the control channels in DL and UL, respectively. We consider the use of 30 kHz SCS as

² The 3.7–3.8 GHz band is considered in some European countries for non-public network deployments [26].

recommended in [20] for industrial environments (we also evaluate the use of 15 and 60 kHz when specifically indicated). There are $N_{UE}=15$ sensors randomly distributed in the work cell, and we consider that they are in Line of Sight with the gNB. The radio channel is characterized by fast-fading and shadowing, and they follow a spatial channel model defined in [21]. Sensors transmit packets with size p_i equal to 10 or 25 bytes in UL to a central monitoring system using configured grant (these packet sizes are typical of closed-loop control applications [22]). The IPv4 header with a value of 22 bytes is added to this packet size, $p_{headers}$. We also consider the use of cyclic redundancy check (CRC) code. All sensors use MCS 12 in MCS table 1 [11]; MCS 12 provides a good trade-off between robustness and transmission rate in the considered scenario. Furthermore, we have use one Multiple-Input Multiple-Output (MIMO) transmission layer (referred to as v). Processing times in the UE and gNB are calculated as indicated in [23] and [11].

We compare the performance achieved with the designed CG scheduling policies when 5G NR OFDMA is used with the performance achieved when the implemented multiple access schemes in 5G-LENA are used (represented as 5GL-TDMA and 5GL-OFDMA, respectively). To make a fair comparison, a First Come First Served scheduler is applied with 5GL-TDMA and 5GL-OFDMA. In this context, the scheduler serves UEs following a first-come, first-served basis, i.e., from UE $_1$ to UE $_{N_{UE}}$. Each UE receives the required number of RBs and OFDM symbols to satisfy its demand. When 5GL-TDMA is used, all UEs will receive $r_i=R_{BW}$, and s_i will be calculated for each UE as $s_i=\lceil d_i/R_{BW} \rceil$ to meet its demand. When 5GL-OFDMA is applied, all UEs will receive $s_i=S_{slot}$ OFDM symbols, and r_i is calculated as $r_i=\lceil d_i/S_{slot} \rceil$.

6. Analytical Validation

In this section, we derive the analytical expressions that model the maximum UL latency experienced by the UEs using CG and the different scheduling policies and multiple access schemes. In this work, the UL latency accounts for the elapsed time from when a packet is created at the RLC layer of a UE until it is received at the RLC layer of the gNB. We compare the results achieved analytically with those achieved by simulation in order to validate the implementation in CG in 5G-LENA.

6.1. Analytical Modeling

This subsection derives the analytical expressions of the maximum UL latency (L_{UL}) experienced by the UEs. We consider that all UEs transmit packets with the same size. Following [24], the latency of a packet transmitted in UL with CG is given by the following components. First, we

need to account for the processing times at the UE and the gNB that represent the time required to generate the packet at the transmitter and decode the data at the receiver, respectively ($t_{UE,tx}$ and $t_{gNB,rx}$). Another latency components are the frame alignment time (t_{fa}) that accounts for the time interval from the creation of a packet until the next transmission opportunity for the Physical Uplink Shared Channel (PUSCH), the waiting time for the resources allocated for the packet transmission (t_w), and the transmission time of the packet (t_{tt}). L_{UL} is then calculated as:

$$L_{UL} = t_{UE,tx} + t_{fa} + t_w + t_{tt} + t_{gNB,rx} \quad (1)$$

The processing time at the transmitter and the receiver ($t_{UE,tx}$ and $t_{gNB,rx}$) are calculated as indicated in [23]. t_{fa} depends on the frame structure, i.e., on the configuration of slots and OFDM symbols within a slot for the transmission of control and data channels for DL and UL transmissions. The waiting time t_w accounts for the time interval that a UE has to wait after t_{fa} for the assigned resources. t_w depends on the way radio resources are allocated to the UEs. Therefore, t_w depends on the multiple access mode and the scheduling policy. The transmission time t_{tt} is equal to the time duration of the OFDM symbols used for the packet transmission, and it can be calculated as $s_i \cdot T_{sym}$, T_{sym} is the duration of a OFDM symbol. T_{sym} depends on the numerology used for the transmission of the packet, and s_i depends on the multiple access mode and scheduling scheme. For numerology 1 with SCS 30 kHz, T_{sym} is equal to 35.67 ms. We calculate t_{fa} , t_w and t_{tt} for the different scheduling policies and multiple access schemes studied in this work.

6.1.1. 5GL-TDMA

5GL-TDMA allocates all RBs in an OFDM symbol to the same UE. As a result, a UE_{*i*} receives $r_i^{5GL-TDMA} = R_{BW}$ RBs and $s_i^{5GL-TDMA} = \lceil d_i / R_{BW} \rceil$ OFDM symbols. R_{BW} depends on the bandwidth and is given in [19].

t_{tt} for a UE_{*i*} can be calculated as $\lceil d_i / R_{BW} \rceil \cdot T_{sym}$, where d_i is the number of radio resources demanded by UE_{*i*}. d_i can be calculated as a function of the packet size (p_i) and the MCS used to transmit the packet as:

$$d_i = \left\lceil \frac{(tbs_i(p_i + p_{headers}) + CRC)}{R \cdot Q_m \cdot v \cdot N_{sc,RB}} \right\rceil \quad (2)$$

In (2), $tbs_i(p_i + p_{headers})$ represents the smallest transport block size from the available values given in [25] that can be used to transmit $p_i + p_{headers}$ bits. Q_m is the modulation order, R is the code rate and v is the number of MIMO transmission layers. The waiting time for the last UE served (the one that experiences the highest latency) is equal to the transmission time required by the other $N_{UE}-1$ UEs requesting resources. Therefore, we can calculate $t_w + t_{tt}$ as:

$$t_w + t_{tt} = \sum_{i=1}^{N_{UE}} \left\lceil \frac{d_i}{R_{BW}} \right\rceil \cdot T_{sym} \quad (3)$$

If all UEs transmit packets of the same size, (3) can be expressed as:

$$t_w + t_{tt} = N_{UE} \cdot \left\lceil \frac{d_i}{R_{BW}} \right\rceil \cdot T_{sym} \quad (4)$$

t_{fa} accounts for the delay introduced by the transmission of other channels (control channels in UL and DL -PUCCH or PDCCH- or the transmission of the PDSCH). We consider that the first and last OFDM symbols of a slot are reserved for the transmission of control channels and 12 OFDM symbols are used for data transmission in UL. To calculate t_{fa} , we need to know how many slots are needed to allocate resources for all UEs, which is represented as n_{slot} , and is calculated as:

$$n_{slot} = \left\lceil \frac{\sum_{i=1}^{N_{UE}} s_i^{5GL-TDMA}}{12} \right\rceil = \left\lceil \frac{N_{UE} \cdot s_i^{5GL-TDMA}}{12} \right\rceil \quad (5)$$

The first and last OFDM symbols in each slot are dedicated for control channels transmissions. Then, t_{fa} is calculated as:

$$t_{fa} = (2 \cdot n_{slot} - 1) \cdot T_{sym} \quad (6)$$

Using (4), (5) and (6), the maximum latency experienced by UEs using 5GL-TDMA is calculated as:

$$L_{UL} = t_{UE,tx} + (2 \cdot n_{slot} - 1 + N_{UE}) \cdot \left\lceil \frac{d_i}{R_{BW}} \right\rceil \cdot T_{sym} + t_{gNB,rx} \quad (7)$$

6.1.2. 5GL-OFDMA

5GL-OFDMA allocates the same RB in all OFDM symbols within a slot to the same UE. 5GL-OFDMA then allocates $r_i^{5GL-OFDMA} = \lceil d_i / S_{slot} \rceil$ RBs in $s_i^{5GL-OFDMA} = S_{slot}$ OFDM symbols for each UE_{*i*} (d_i is calculated in (2)). The latency $t_{fa} + t_w + t_{tt}$ for 5GL-OFDMA is calculated as the time needed to transmit n_{slot} slots minus the time duration of the last OFDM symbol. n_{slot} is the number of slots used to transmit the packets of all UEs. $t_{fa} + t_w + t_{tt}$ is then calculated as:

$$t_{fa} + t_w + t_{tt} = n_{slot} \cdot T_{slot} - T_{sym} = (14 \cdot n_{slot} - 1) \cdot T_{sym} \quad (8)$$

In (8), T_{slot} is the time duration of a slot, that is equal to $14 \cdot T_{sym}$. n_{slot} in (8) is calculated as:

$$n_{slot} = \left\lceil \sum_{i=1}^{N_{UE}} r_i^{5GL-OFDMA} / R_{BW} \right\rceil = \left\lceil \frac{N_{UE} \cdot r_i^{5GL-OFDMA}}{R_{BW}} \right\rceil \quad (9)$$

Using (9) and (10), the maximum latency experienced by UEs using 5GL-OFDMA is calculated as:

$$L_{UL} = t_{UE,tx} + (14 \cdot n_{slot} - 1) \cdot T_{sym} + t_{gNB,rx} \quad (10)$$

6.1.3. Sym-OFDMA

Sym-OFDMA allocates to each UE_{*i*} the number of RBs necessary to satisfy d_i in the minimum number of OFDM symbols possible. We can then distinguish two cases. When $d_i > R_{BW}$, the UE_{*i*} receives $r_i^{Sym-OFDMA} = R_{BW}$ RBs in $s_i^{Sym-OFDMA} = \lceil d_i / R_{BW} \rceil$ consecutive symbols. When $d_i \leq R_{BW}$, Sym-OFDMA allocates $r_i^{Sym-OFDMA} = d_i$ RBs and $s_i^{Sym-OFDMA} = 1$ to UE_{*i*}. In this case, several UEs can share the RBs in the same OFDM symbol. The number of UEs sharing RBs in the same OFDM symbol is given by $\lfloor R_{BW} / d_i \rfloor$ when all UEs demand the same number d_i of RBs. We can then calculate the number of OFDM symbols n_{sym} needed to serve all UEs as:

$$n_{sym} = \begin{cases} \frac{N_{UE}}{\lfloor R_{BW} / d_i \rfloor}, & d_i \leq R_{BW} \\ \lceil \frac{d_i}{R_{BW}} \rceil \cdot N_{UE}, & d_i > R_{BW} \end{cases} \quad (11)$$

Using (11), the number of slots needed to serve all UEs is equal to $n_{slot} = \lceil n_{sym} / 12 \rceil$; each slot has 12 OFDM symbols for UL data transmission. Considering that the first and last OFDM symbol within slots are used for control channels, $t_{fa} + t_w + t_{tt}$ can be calculated as:

$$t_{fa} + t_w + t_{tt} = (2 \cdot n_{slot} - 1 + n_{sym}) \cdot T_{sym} \quad (12)$$

The maximum latency experienced using Sym-OFDMA is calculated as:

$$L_{UL} = t_{UE,tx} + (2 \cdot n_{slot} - 1 + n_{sym}) \cdot T_{sym} + t_{gNB,rx} \quad (13)$$

6.1.4. RB-OFDMA

RB-OFDMA establishes that each UE_{*i*} has to receive at least r_{min} RBs. Considering this constraint, it distributes the R_{BW} RBs in a symbol among the maximum number of UEs. The maximum number of UEs that can share the RBs in an OFDM symbol is given by $n_{UE,1} = \lfloor R_{BW} / r_{min} \rfloor$. In this context, the N_{UE} UEs are divided in $\lfloor N_{UE} / n_{UE,1} \rfloor$ groups of $n_{UE,1}$ UEs that receive $r_i^{RB-OFDMA(1)} = r_{min}$ RBs in $s_i^{RB-OFDMA(1)} = \lceil d_i / r_{min} \rceil$

OFDM symbols, and one last group with $n_{UE,2} = N_{UE} - \lfloor N_{UE} / n_{UE,1} \rfloor \cdot n_{UE,1}$ UEs that receive $r_i^{RB-OFDMA(2)} = \lfloor R_{BW} / r_{min} \rfloor / n_{UE,2} \cdot r_{min}$ RBs in $s_i^{RB-OFDMA(2)} = \lceil d_i / r_i^{RB-OFDMA(2)} \rceil$ OFDM symbols. We can then calculate the number n_{sym} of OFDM symbols necessary to serve all UEs as:

$$n_{sym} = \lfloor N_{UE} / n_{UE,1} \rfloor \cdot s_i^{RB-OFDMA(1)} + s_i^{RB-OFDMA(2)} \quad (14)$$

Using (14), the number of slots needed to serve all UEs is calculated as $n_{slot} = \lceil n_{sym} / 12 \rceil$. Considering that the first and last OFDM symbols within slots are used for control channels, $t_{fa} + t_w + t_{tt}$ can be calculated using (12) as $(2 \cdot n_{slot} - 1 + n_{sym}) \cdot T_{sym}$. The maximum latency experienced using RB-OFDMA is calculated as:

$$L_{UL} = t_{UE,tx} + t_{gNB,rx} + \left(2 \cdot n_{slot} - 1 + \left\lfloor \frac{N_{UE}}{n_{UE,1}} \right\rfloor \cdot s_i^{RB-OFDMA(1)} + s_i^{RB-OFDMA(2)} \right) \cdot T_{sym} \quad (15)$$

6.2. Validation

Figure 7 compares the maximum latency experienced in UL transmissions obtained analytically and through simulations when using CG with 5GL-TDMA, 5GL-OFDMA, Sym-OFDMA, and RB-OFDMA for different bandwidth values (BW) when packets size is equal to 10 bytes and slot format 1D13U is used. The figure clearly shows that the simulated and analytical results precisely match for all the multiple access schemes and scheduling policies evaluated. It is important to note that the maximum latency obtained with Sym-OFDMA and RB-OFDMA is equal to or lower than the maximum latency experienced with 5GL-TDMA and 5GL-OFDMA for all the evaluated BW values. The same maximum latency is achieved for all BW s when 5GL-TDMA is used. This is because 5GL-TDMA assigns all the RBs in an OFDM symbol to the same UE regardless of the number of RBs available or BW and its RB demand. As a result, 5GL-TDMA uses the same number of OFDM symbols to serve the N_{UE} UEs for all the evaluated BW values, and the latency experienced by the last served UE does not change with BW . When 5GL-OFDMA is used, the maximum latency experienced by a UE decreases a 43.1% when BW increases from 10 to 20 MHz. This is because two slots are needed to allocate resources to all the UEs when $BW=10$ MHz. When BW increases to 20 MHz, the radio resource demand of all UEs can be satisfied with the RBs in one slot. Since each UE receives RBs in all the OFDM symbols dedicated for data within a slot, the maximum latency experienced by a UE remains constant as BW increases above 20 MHz. Both Sym-OFDMA and RB-OFDMA provide the lowest maximum latency values for all the BW evaluated. In addition, the maximum latency experienced with both scheduling policies decreases when BW

increases. This is due to the greater flexibility introduced by OFDMA that allows radio resources to be allocated more efficiently and the experienced latency to be reduced. The performance achieved with both Sym-OFDMA and RB-OFDMA is analyzed more in-depth in the following section.

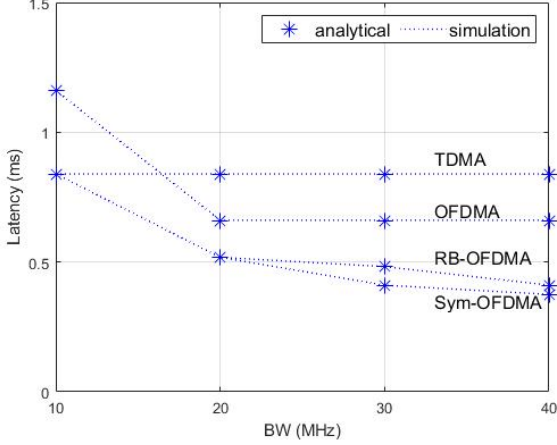


Figure 7. Maximum UL latency as a function of the bandwidth (packet size of 10 bytes).

7. Performance evaluation

First, we compare the latency results obtained when using dynamic scheduling and CG for UL transmissions using 5G-LENA (Table 1). We also compare the latency results obtained with CG using 5G-LENA with the analytical values reported in [23] (third column in Table 1). We consider a scenario with only one UE that transmits empty packets using 2 OFDM symbols. We evaluate the use of numerologies (μ) 0, 1 and 2, which correspond to a subcarrier spacing of 15, 30 and 60 kHz. We consider a slot format 1D13U and $BW=20$ MHz. The results in Table 1 show that the latency results obtained with CG implemented in 5G-LENA are in line with the analytical results presented in 3GPP TR 37.910 [23], which validates the implemented CG in 5G-LENA. Moreover, the latency obtained with configured grant has a reduction of 93.3% compared to the latency obtained with the dynamic scheduler in the case of numerology 0.

Table 1. Latency experienced with Dynamic Scheduling and Configured Grant

μ	Dynamic scheduling	Configured Grant	
		5G-LENA	TR 37.910 [23]
0	7.31 ms	0.49 ms	0.52 ms
1	3.70 ms	0.30 ms	0.30 ms
2	1.90 ms	0.25 ms	0.24 ms

Now, we analyze the latency that can be achieved when the different multiple access schemes and scheduling policies are applied. Figure 8 shows a boxplot of the UL latency experienced by the UEs using CG with 5GL-TDMA, 5GL-OFDMA, Sym-OFDMA and RB-OFDMA when bandwidth is equal to 10, 20 and 40 MHz and packet size is 10 bytes. In Figure 8, the red line within the box represents the average of the experienced latency, and the edges of the box the 10th and 90th percentiles. The crosses represent the minimum and maximum values. At least otherwise indicated, we consider a packet size of 10 bytes and slot format 1D13U. Figure 9 depicts the number of radio resources used with the different multiple access modes and scheduling policies calculated with respect to the number of radio resources used by 5GL-TDMA. Figure 8 shows that Sym-OFDMA and RM-OFDMA equal or reduce the maximum and average latency experienced by the UEs for all the evaluated BW values compared with 5GL-OFDMA and 5GL-TDMA. This is due to a more efficient use of radio resources, as shown in Figure 9. When the bandwidth is low ($BW=10$ MHz), both Sym-OFDMA and RM-OFDMA achieve similar latency results to that achieved with 5GL-TDMA. 5GL-TDMA assigns all the RBs in a symbol to the same UE. In this case, the number of RBs needed to transmit 10-byte packets is equal to the number of RBs available in the 10 MHz bandwidth. Sym-OFDMA then allocates all the RBs in a symbol to a UE, achieving the same latency performance as 5GL-TDMA. Figure 8 also shows that both 5GL-TDMA and Sym-OFDMA use the same amount of radio resources. When $BW=10$ MHz, RB-OFDMA allocates RBs in two consecutive symbols to each UE, and the RBs in a symbol are shared by two UEs. As a result, the maximum latency experienced with RB-OFDMA is the same as with 5GL-TDMA and Sym-OFDMA, as shown in Figure 8. Figure 9 shows that RB-OFDMA also uses the same number of radio resources than 5GL-TDMA and Sym-OFDMA. 5GL-OFDMA provides the largest latency values when the bandwidth is 10 MHz. 5GL-OFDMA allocates RBs in all symbols within a slot to UEs. When bandwidth is equal to 10 MHz, only 8 of the 15 UEs can receive resources in the first slot after the packets are generated, and they experience a latency of 0.65 ms. The rest of the UEs receive resources in the next slot and experience a latency equal to 1.15 ms. Figure 9.a shows that 5GL-OFDMA uses a 40% more of radio resources than 5GL-TDMA, Sym-OFDMA and RB-OFDMA.

When the bandwidth increases from 20 to 40 MHz, 5GL-OFDMA reduces the maximum latency experienced compared with 5GL-TDMA. Figure 8 shows that all UEs experience the same latency when BW is equal to 20 and 40 MHz. This happens because all UEs share RBs in all the OFDM symbols of the first slot after the packets are generated. Sym-OFDMA and RB-OFDMA achieve the lowest latency for the UEs. Furthermore, both Sym-OFDMA and RB-OFDMA use a lower number of radio resources to serve the N_{UE} UEs than 5GL-TDMA and 5GL-OFDMA (Figure 9). Sym-OFDMA allows several UEs share the RBs

in the same OFDM symbol. As BW and the number of available RBs increase, more UEs receive RBs in the same OFDM symbol. Sym-OFDMA then requires a lower number of OFDM symbols to serve all UEs compared with 5GL-TDMA. As a result, the latency experienced by the UEs decreases. Figure 8 also shows that the maximum latency experienced with RB-OFDMA also reduces when the bandwidth increases. However, the minimum and average latency experienced increases when bandwidth increases from 20 to 40 MHz. This is due to the different number of OFDM symbols allocated to the UEs when BW is equal to 20 and 40 MHz, respectively. When $BW=20$ MHz, each UE receives RBs in only one OFDM symbol, and the RBs in a symbol are shared by 2 UEs. When bandwidth is equal to 40 MHz, RB-OFDMA allocates RBs in 5 consecutive OFDM symbols to each UE, and the RBs in a symbol are shared by all the UEs.

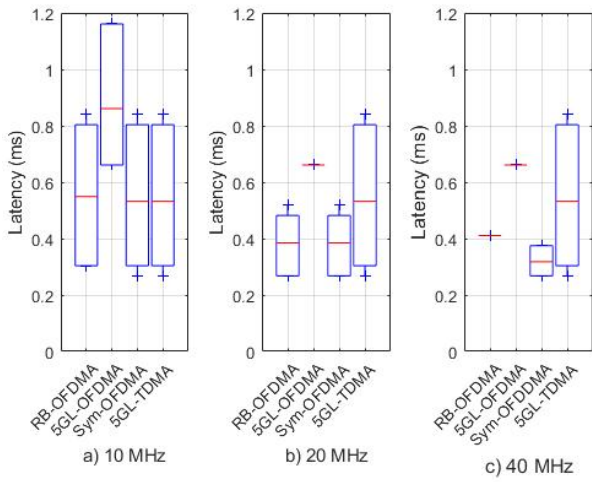


Figure 8. UL latency experienced as a function of the bandwidth (packet size of 10 bytes).

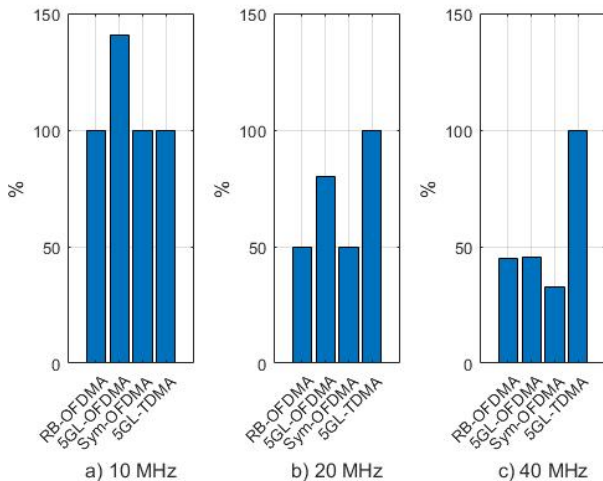


Figure 9. Percentage of radio resources used for the transmission of packets with respect to 5GL-TDMA (packet size of 10 bytes).

Figure 10 shows the boxplot of the UL latency experienced by the UEs using CG with 5GL-TDMA, 5GL-OFDMA, Sym-OFDMA and RB-OFDMA when packets of 10 and 25 bytes are transmitted, respectively, and considering $BW=20$ MHz, and slot format 1D13U. Figure 10 shows that the latency experienced by the UEs increases with the packet size for Sym-OFDMA and RB-OFDMA, while it remains constant for 5GL-TDMA and 5GL-OFDMA. This is the case because 5GL-TDMA and 5GL-OFDMA allocate more radio resources than demanded by each UE when 10 bytes of data are transmitted per packet. The number of allocated radio resources is enough to satisfy the radio resource demand when the packet size increases to 25 bytes. Therefore, the experienced UL latency remains constant with 5GL-TDMA and 5GL-OFDMA because they allocate the same radio resources to UEs when packet size is 10 and 25 bytes. On the other hand, Sym-OFDMA and RB-OFDMA allocate to each UE a number of radio resources more adjusted to their demands thanks to the flexibility provided by 5G NR OFDMA. For that reason, the number of allocated radio resources to each UE increases when packet size increases. This also results in the increase of the UL latency experienced by the UEs. However, it is important to highlight that the maximum UL latency experienced with Sym-OFDMA and RB-OFDMA is always lower than the experienced with 5GL-TDMA and 5GL-OFDMA, respectively. In the case of Sym-OFDMA, the number of available RBs is not enough to satisfy the demand of more than one UE, and each UE receives RBs in different OFDM symbols. As a result, Sym-OFDMA and 5GL-TDMA achieve the same latency performance. However, Sym-OFDMA only uses the 66% of the radio resources used by 5GL-TDMA, and the non-allocated radio resources could be used by other UEs. RB-OFDMA has higher flexibility than Sym-OFDMA since it can allocate any number of RBs and OFDM symbols to each UE; the number of OFDM symbols is always 1 with Sym-OFDMA if the radio resource demand of the UE can be satisfied with the available

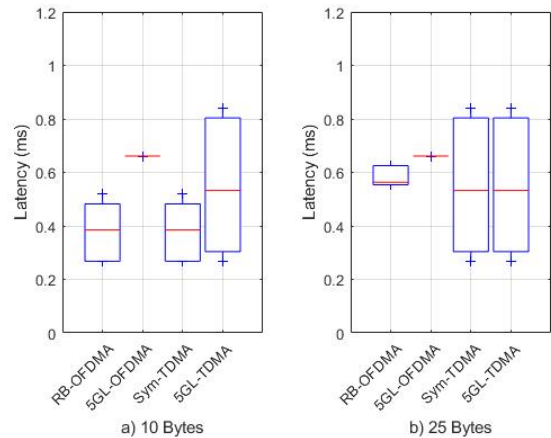


Figure 10. UL latency experienced as a function of the packet size ($BW=20$ MHz).

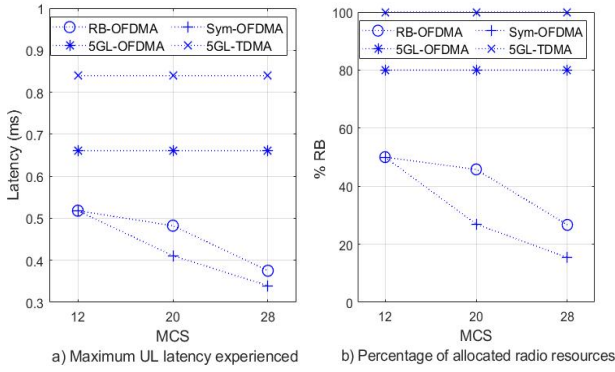


Figure 11. Performance as a function of the MCS ($BW = 20$ MHz, packet size = 10 bytes).

RBs in an OFDMA symbol. Thanks to this, it achieves a lower maximum UL latency when packet size is equal to 25 bytes.

Now, we evaluate the impact of the MCS used for the packet transmissions. Figure 11 shows the maximum UL latency experienced by the UEs and the percentage of allocated radio resources using CG with 5GL-TDMA, 5GL-OFDMA, Sym-OFDMA and RB-OFDMA when MCS 12, 20 and 28 are used and $BW=20$ MHz and packets of 10 bytes are transmitted. The percentage of radio resources allocated is calculated with respect to the number of radio resources used by 5GL-TDMA. Figure 11.a shows that Sym-OFDMA and RB-OFDMA using 5G NR OFDMA reduce the maximum latency experienced by the UEs for all the evaluated MCSs compared with 5GL-OFDMA and 5GL-TDMA. This is thanks to the most efficient use of radio resources, as shown in Figure 11.b. When MCS increases, a lower number of RBs are demanded by each UE to transmit their packets. Sym-OFDMA and RB-OFDMA adjust the number of allocated resources to the UEs demand exploiting the flexibility offered by OFDMA. However, 5GL-TDMA and 5GL-OFDMA maintain the same radio resource allocation for all MCS values evaluated due to the constraints introduced by the multiple access schemes implemented in 5G-LENA. As a result, Sym-OFDMA and RB-OFDMA reduce the number of allocated radio resources and the maximum experienced UL latency compared with 5GL-TDMA and 5GL-OFDMA. For example, Sym-OFDMA and RB-OFDMA reduce the maximum UL latency by 48.63% and 43.22%, respectively, compared with 5GL-OFDMA when MCS 28 is used. These results are achieved using only a 80.7% and 66.7% of the radio resources used by 5GL-OFDMA. Compared with 5GL-TDMA, Sym-OFDMA and RB-OFDMA reduce the maximum UL latency a 59.5% and 55.3%, respectively, using only 15.38% and 26.67% of the radio resources.

Finally, we also evaluate how CG with the different multiple access schemes and scheduling policies adapts the radio resource allocation when the slot format changes. Figure 12 shows the boxplot of the UL latency experienced by UEs when different slot formats are used, $BW=20$ MHz, and packet size is equal to 10 bytes. Each slot format reserves a different

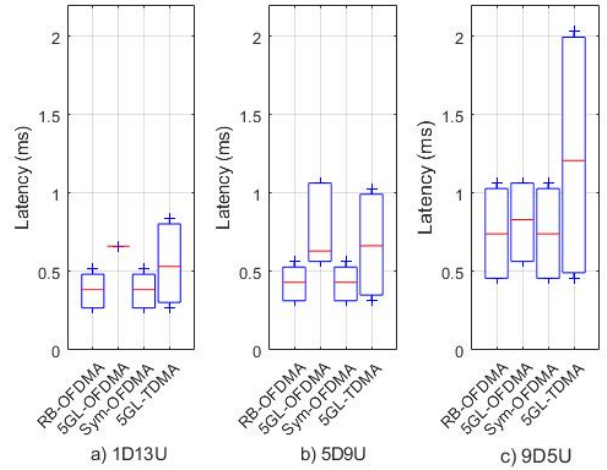


Figure 12. Latency experienced with the different schemes as a function of the slot format ($BW = 20$ MHz, packet size = 10 bytes).

number of OFDM symbols for UL transmissions. Particularly, we consider that the last 13, 9 and 5 OFDM symbols within a slot can be used for UL transmissions (the rest of OFDM symbols within a slot are reserved for DL transmissions). Figure 12 shows that, as expected, the latency increases for all multiple access schemes and scheduling policies when the number of OFDM symbols reserved for UL transmissions within a slot decreases. Sym-OFDMA and RB-OFDMA always provide the lowest latency values thanks to the higher flexibility offered by OFDMA multiple access scheme. 5GL-TDMA is the one for which the experienced UL latency increases more. This is because 5GL-TDMA requires a larger number of slots to serve all the UEs as the number of OFDM symbols reserved for UL within a slot decreases.

8. Conclusions

This paper has presented a detailed description of the first implementation of configured grant scheduling in an open source 5G NR simulator (to the best of the author's knowledge), in particular in 5G-LENA. The code of configured grant is publicly available in [7]. Configured grant pre-allocates radio resources to the UEs and avoids the signaling exchange between the UE and the gNB to request/inform about the allocated radio resources reducing the latency of the transmission. Configured grant is key for the support of time-critical services in 5G networks. This work is a valuable contribution since the availability of simulation tools that accurately model all the functionalities of 5G NR and, in particular, configured grant, is fundamental for the research in 5G and beyond networks supporting time-critical services. In particular, we have presented the new functionalities and modifications included at the MAC and PHY layers of 5G-LENA to integrate configured grant in the simulator. To accurately model the high flexibility offered by 5G NR in the radio resource allocation process, we have

also implemented the 5G NR OFDMA in the simulator that allows radio resources to be shared simultaneously in time and frequency by different UEs. Using OFDMA multiple access scheme, it is possible to transmit using any number of OFDM symbols. The latency results achieved with configured grant in 5G-LENA match with the latency values reported in previous analytical studies, which validates the implementation of configured grant in 5G-LENA.

We have also implemented two scheduling policies that are applied with configured grant and OFDMA to demonstrate the flexibility and capabilities of 5G NR to support time-critical services. The proposed scheduling policies exploit the flexibility offered by OFDMA to guarantee low latencies and efficient use of radio resources. We have considered a case study where a 5G NR cell covers an industrial scenario where a closed-loop control application demands for low latency communications. The results have shown that the use of CG with the proposed scheduling policies and OFDMA reduces the maximum latency experienced by UEs by up to 48.63% compared to the latency experienced when the multiple access schemes previously implemented in 5G-LENA are used. This result is achieved using a 80.7% less radio resources. The results have shown that the use of scheduling policies that make efficient use of radio resources is more critical the smaller the size of the packets to be transmitted.

Acknowledgments

This work has been funded by MCIN/AEI/10.13039/501100011033 through the project PID2020-115576RB-I00, and by European Union's Horizon Europe Research and Innovation programme under Grant Agreement No 101057083.

References

- [1] 5G-ACIA, "5G for Connected Industries and Automation" 2019.
- [2] 5G-ACIA, "Key 5G Use Cases and Requirements" 2020.
- [3] S. Zeb, A. Mahmood, S. A. Hassan, M. J. Piran, M. Gidlund, and M. Guizani, "Industrial digital twins at the nexus of NextG wireless networks and computational intelligence: A survey" *J. Netw. Comput. Appl.*, vol. 200, p. 103309, Apr. 2022.
- [4] E. Dahlman and S. Parkvall, "NR - The new 5G radio-access technology" *IEEE 87th Vehicular Technology Conference*, vol. 2018-June, pp. 1–6, 2018.
- [5] N. Patriciello, S. Lagen, B. Bojovic, and L. Giupponi, "An E2E Simulator for 5G NR Networks" *Simul. Model. Pract. Theory*, vol. 96, Nov. 2019.
- [6] ns-3 | a discrete-event network simulator for internet systems: Available at: <https://www.nsnam.org/>.
- [7] Open-source implementation of Configured Grant in 5G-LENA: Available at: <https://gitlab.com/ns-3-dev-nr-configuredgrant/nr/-/tree/5g-lena-cg-v2.1.y>.
- [8] Open source implementation ns-3 (updated to use with configured-grant): Available at: <https://gitlab.com/ns-3-dev-nr-configuredgrant/ns-3-dev/-/tree/ns-3.36-cg>.
- [9] 3GPP TSG RAN, "Physical channels and modulation" Rel. 16; TS 38.211, v16.7.0, 2021.
- [10] A. A. Zaidi, R. Baldemair, M. Andersson, S. Faxer, V. Moles-cases, and Z. Wang, "The 5G NR Physical Layer Design" *Ericsson Technol. Rev.*, vol. 1, 2017.
- [11] 3GPP TSG RAN, "Physical layer procedures for data" Rel. 16; TS 38.214, v16.1.0, 2020.
- [12] 3GPP TSG RAN "NR and NG-RAN Overall Description" Rel. 16; TS 38.300, v16.7.0, 2021.
- [13] B. Bojović, S. Lagén, and L. Giupponi, "Realistic beamforming design using SRS-based channel estimate for ns-3 5G-LENA module" *ACM Int. Conf. Proceeding Ser.*, pp. 81–87, 2021.
- [14] B. Bojovic, Z. Ali, and S. Lagen, "ns-3 and 5G-LENA Extensions to Support Dual-Polarized MIMO," 2022.
- [15] T. Zugno, M. Polese, N. Patriciello, B. Bojović, S. Lagen, and M. Zorzi, "Implementation of a Spatial Channel Model for ns-3" *ACM Int. Conf. Proceeding Ser.*, pp. 49–56, Feb. 2020.
- [16] K. Koutlia, B. Bojovic, Z. Ali, and S. Lagén, "Calibration of the 5G-LENA system level simulator in 3GPP reference scenarios" *Simul. Model. Pract. Theory*, vol. 119, p. 102580, Sep. 2022.
- [17] N. Patriciello, S. Lagen, L. Giupponi, and B. Bojovic, "An improved MAC layer for the 5G NR ns-3 module" *ACM Int. Conf. Proceeding Ser.*, no. November, pp. 41–48, 2019.
- [18] 3GPP TSG RAN, "Radio Resource Control (RRC) protocol specification" Rel. 16; TS 38.331, v16.6.0. 2021.
- [19] 3GPP TSG RAN, "Base Station (BS) radio transmission and reception" Rel. 17; TS 38.104, v17.4.0, 2021.
- [20] 3GPP TSG RAN, "Study on physical layer enhancements for NR ultra-reliable and low latency case (URLLC)" Rel. 16; TR 38.824, v16.0.0, 2019.
- [21] 3GPP TSG RAN, "Study on channel model for frequencies from 0.5 to 100 GHz" Rel. 17; TR 38.901, v17.0.0, 2022.
- [22] K. Montgomery, R. Candell, Y. Liu, and M. Hany, "Wireless User Requirements for the Factory Workcell NIST Advanced Manufacturing Series 300-8 Wireless User Requirements for the Factory Workcell," *Adv. Manuf. Ser. (NIST AMS)*.
- [23] 3GPP TSG RAN, "Study on self evaluation towards IMT-2020 submission" Rel. 16; TR 37.910, v16.1.0, 2021.
- [24] M. C. Lucas-Estañ *et al.*, "An Analytical Latency Model and Evaluation of the Capacity of 5G NR to Support V2X Services using V2N2V Communications", pre-print, Dec. 2021. Available at: t.ly/xOEw.
- [25] 3GPP TSG RAN, "Medium Access Control (MAC) protocol specification" Rel. 16; TS 38.321, v16.6.0, 2021.
- [26] European 5G Observatory (2020), "5G private licences spectrum in Europe." Available at: <https://5gobservatory.eu/5g-private-licences-spectrum-in-europe/>.